USP14 regulates ATF2/PIK3CD axis to promote microvascular endothelial cell proliferation, migration and angiogenesis in diabetic retinopathy

Fu-Tao He
Hainan West Central Hospital
Xiao-Lin Fu (xiaolinfu12345@163.com)
Hainan West Central Hospital
Mo-Han Li
Hainan West Central Hospital
Chun-Yan Fu
Hainan West Central Hospital
Jian-Zhi Chen
Hainan West Central Hospital

Research Article

Keywords: diabetic retinopathy, angiogenesis, USP14 ATF2 PIK3CD

Posted Date: August 1st, 2022

DOI: https://doi.org/10.21203/rs.3.rs-1892956/v1

Additional Declarations: No competing interests reported.

Version of Record: A version of this preprint was published at Biochemical Genetics on March 20th, 2023. See the published version at https://doi.org/10.1007/s10528-023-10358-0.

Abstract

Background

Diabetic retinopathy (DR) is the foremost cause of blindness in diabetic patients. However, the pathogenesis of DR is complex, and no firm conclusions have been drawn so far. It has become a hot spot in ophthalmology research to deeply study the mechanism of DR pathological changes and find effective treatment options.

Methods

Human retinal microvascular endothelial cells (HRMECs) were induced using high glucose (HG) to construct DR cell model. CCK-8 assay was utilized to ascertain the viability of HRMECs. Transwell assay was manipulated to ascertain the migration ability of HRMECs. Tube formation assay was utilized to ascertain the angiogenesis ability of HRMECs. The expressions of USP14, ATF2 and PIK3CD were ascertained by qRT-PCR assay and Western blot analysis. Immunoprecipitation (IP) was manipulated to identify the relationship of USP14 and ATF2. To explore the regulatory relationship between ATF2 and PIK3CD by chromatin immunoprecipitation (ChIP) assay, along with dual-luciferase reporter gene assay.

Results

The proliferation, migration and angiogenesis of HRMECs were enhanced after high glucose treatment, and the expressions of USP14, ATF2 and PIK3CD were significantly up-regulated. Knockdown of USP14 or ATF2 inhibited cell proliferation, migration and angiogenesis in HG-induced HRMECs. USP14 regulated the expression of ATF2, and ATF2 promoted PIK3CD expression. PIK3CD overexpression attenuated the inhibitory effectiveness of USP14 knockdown on proliferation, migration and angiogenesis of DR cell model.

Conclusion

Here we revealed that USP14 regulated the ATF2/PIK3CD axis to promote proliferation, migration and angiogenesis in HRMECs upon high glucose.

Introduction

Diabetes is a disease with pathological changes of microvessels in various organs of the body caused by disturbance of glucose metabolism, and the main manifestations in the ocular region are the formation of microhemangioma, neovascularization, hemorrhage, organization, fibrous hyperplasia and contracture, and finally traction of the retina leads to retinal hole and detachment (1). Therefore, diabetic retinopathy (DR) is the most serious blindness ophthalmopathy. Recently, the number of DR patients has increased

enormously, and the problems caused by DR have attracted more and more attention (2). At present, anti-vascular endothelial growth factor (VEGF) therapy is the mainstream treatment for DR, but it requires repeated intravitreal injections and is only effective for middle-advanced DR, so there are limitations (3). Before the retinal microvascular damage occurs in diabetic patients, pathophysiological changes in the retina have already occurred, which affect their visual function, but there are few treatment measures for these early-stage damages (4, 5). Thence, exploring the molecular biology alteration mechanism of DR and finding potential therapeutic methods have invaluable significance.

As an important component of the ubiquitin-proteasome system (UPS), deubiquitinating enzyme (DUB) regulates the ubiquitination process of target proteins and has a regulatory effect on the function and degradation of proteins (6). Ubiquitin-specific protease 14 (USP14) is an important deubiquitinating enzyme that regulates protein stability (7). USP14 is involved in diseases such as signal transduction, neurological diseases, glucose and lipid metabolism, and tumorigenesis, which makes it a promising drug target (8–10). According to Fu et al. reported that USP14 expression was significantly up-regulated in diabetic rats retina and HG-stimulated Müller cells, and the lncRNA OGRU/miR-320/USP14 axis participated in the progression of DR by regulating inflammation and oxidative stress (11). Regardless, there is still a gap on the role of USP14 in angiogenesis and its related mechanisms in the development of DR, and further investigation is needed.

Activating transcription factor 2 (ATF2) pertains to the basic leucine zipper transcription factor family, which binds to DNA in the form of homodimers or heterodimers and regulates the transcriptional activity of target genes (12). Lin et al. confirmed that the p38 MAPK/ATF2 signaling pathway possessed an essential function in regulating cognitive function and apoptosis in diabetes (13). Furthermore, Shao et al. revealed that ATF2 expression was enhanced in diabetic mouse retina, and miR-451a/ATF2 was involved in retinal pigment epithelial cell proliferation and migration by regulating mitochondrial function (14). However, there is a lack of research on the role of ATF2 in promoting angiogenesis in DR. Interestingly, Geng et al. demonstrated that USP14 deubiquitinated and activated ATF2 in prostate cancer, stabilizing its expression (15). Therefore, we can't help but conjecture that USP14 participates in DR by regulating ATF2 expression.

Phosphoinositide-3 kinase catalytic subunit δ (PI3Kδ, or PIK3CD) is an important regulator of cell growth (16). The research that PI3Kδ is involved in diabetes-related diseases has long been reported (17). Moreover, PI3Kδ was up-regulated in HG-induced human retinal microvascular endothelial cells (HRMECs), and promoted cell proliferation, migration and angiogenesis by regulating Akt pathway activation in vascular endothelial cells, and inhibiting PI3Kδ expression significantly attenuated pathological retinal angiogenesis (18). According to Jaspar prediction, it was found that ATF2 had a binding site for PIK3CD, which has not yet been reported. From this we speculate that ATF2 regulated PIK3CD expression, thus affecting the development of DR.

Therefore, the purpose of this study is to confirm that USP14 promoted the proliferation, migration and angiogenesis of HG-induced HRMECs by regulating the ATF2/PIK3CD axis and to contribute a

newfangled perspective for the development of effective treatment of diabetic retinopathy.

Material And Methods

DR cells model construction

Human retinal microvascular endothelial cells (HRMECs) were obtained from Procell Life Science Technology Co,.Ltd. (Wuhan, China). HRMECs was cultured in Endothelial medium (ECM, Solarbio, Beijing, China) with 5% fetal bovine serum (FBS, Beyotime, Shanghai, China), 1% endothelial cell growth supplement (Beyotime) and 1% penicillin/streptomycin solution (Beyotime) in 37 ^{O}C and 5% CO_2. HRMECs in the logarithmic growth phase were taken for subsequent experimentations. HRMECs in high glucose (HG) group were cultured in 30 mmol/L glucose medium for 48 h, and the cells in the Normal group were cultured in a 5.5 mmol/L glucose medium. In the Mannitol group, cells were cultured in 5.5 mmol/L glucose + 24.5 mmol/L mannitol medium.

Cell transfection

Short hairpin RNA USP14 (sh-USP14), short hairpin RNA ATF2 (sh-ATF2), PcDNA3.1-USP14 (oe-USP14) plasmid, PcDNA3.1-ATF2 (oe-ATF2) plasmid, PcDNA3.1-PIK3CD (oe-PIK3CD) plasmid and corresponding negative control (NC) were obtained from Santa Cruz Biotechnology (Shanghai) Co., Ltd (Shanghai, China). On the authority of the directions of Lipofectamine 3000 transfection reagent (Invitrogen, NY, USA), above plasmids were transfected into cells for 48 h.

Western blot

HRMECs were lysed with RIPA lysis buffer (Beyotime) to obtain the total protein, along with protein concentration was measured with BCA protein quantitative kit (Beyotime). Appropriate protein dosages were disunited by sodium dodecyl sulfate-polyacrylamide gel (SDS-PAGE) electrophoresis along with moved to PVDF membrane. 5% skim milk was sealed for 2 h, and primary antibody diluent of corresponding protein was incubated in 4 ^{O}C overnight. Thenceforth, the secondary antibody dilution was nurtured at ambient temperature for 2 h. Thenceforth the bands were nurtured with ECL luminescence solution (Thermo Fisher, MA, USA) and placed in chemiluminescence imaging system for exposure development. The relative expression of each protein was deconstructed by ImageJ software. The antibody information was as demonstrated: USP14 (ab246010, 1/2000), ATF2 (ab32160, 1/1000), PIK3CD (ab32401, 1/500), and GADPH (ab8245, 1/1000).

Quantitative real-time PCR

Total RNA of HRMECs was obtained on the basis of the standard procedure described in the instruction of TRIzol reagent (Invitrogen, MA, USA). RNA concentration were confirmed by ultraviolet spectrophotometer. Subsequently, the first strand cDNA was synthesized by reverse transcription accordant with the guidelines of the reverse transcription kit (Biosystems, Shanghai, China). Real-time

PCR was manipulated utilizing PCR SYBR (TaKaRa, Tokyo, Japan) Green method. The gene expression was evaluated by $2^{-\Delta\Delta Ct}$ method. The primers information is as demonstrated:

USP14: (F) 5'-TATGCAGGTGCCTTGAGAGC-3',

(R) 5'-TTTCTCGGCAAACTGTGGGA-3';

ATF2: (F) 5'-TTATCCCCTCTTGCAACACC-3',

(R) 5'-TGCTGGACGAACAATAGCTG-3';

PIK3CD: (F) 5 -CATATGTGCTGGGCATTGGC-3',

(R) 5'-TTTCACAGTAGCCCCGGAAC-3',

GAPDH: (F) 5'-CTGACTTCAACAGCGACACC-3',

(R) 5'-GTGGTCCAGGGGTCTTACTC-3'.

Cell Counting Kit-8 (CCK-8) assay

HRMECs were grown logarithmically at a cell density of 5×10^3 cells per well in 96-well culture plates. The 96-well plates were incubated in a 37 ^oC incubator with 5% CO_2 for 24 h. Therewith, adding 10 μL of CCK-8 solution (Beyotime) to each well, incubating for 4 h, and recording the absorbance at 450 nm wavelength with enzyme labeling instrumen (BioTek, VT, USA).

Immunoprecipitation (IP)

HRMECs was lysed with RIPA lysis solution (Beyotime). The cleavage products were centrifuged in 4 ^oC, and the cleavage products were collected. Appropriate amount of cleavage products were directly detected by Western blot to ascertain the expression of USP14 and ATF2 proteins as input, and the rest of the cleavage products were incubated overnight with anti-USP14 or anti-ATF2 antibodies. After incubation, protein G beads (Santa Cruz) were added to incubate for 4 h, and then the precipitated protein G beads were collected by centrifugation. Proteins on the beads were eluted, and the ATF2 and USP14 proteins were detected by western blot.

Transwell assay

HRMECs (2×10^5 cells) in logarithmic growth phase were suspended in 200 μL serum-free medium, and the cell suspension was added to upper chamber, and 600 μL medium with FBS was added to lower chamber. After 24 h of culture, the HRMECs were fixed with 4% paraformaldehyde and stained with crystal violet solution. Randomly select 5 visible points under the microscope to take pictures and count. The average number of cells that penetrated into lower chamber was used as the experimental result.

Tube formation assay

200 μL of Matrigel matrix glue (BD, NJ, USA) was added to the 24-well plate and put into 37 ^{o}C, 5% CO_2 incubator for solidification. The cells cultured for 48 h in each group were prepared into 2 × 10^5 / mL suspension with ECM medium and added to the 24-well plate containing Matrigel matrix glue according to 1 mL/ well. The cells were cultured in 37 ^{o}C, 5% CO_2 incubator. After 8 h, the capillary structure was photographed. ImageJ software was manipulated to examine the capillary-like structures.

Dual-luciferase reporter gene assay

Jaspar (https://jaspar.genereg.net/) was used to speculate the binding of ATF2 to PIK3CD. The 3'-UTR cDNA sequences of PIK3CD-WT and PIK3CD-MUT were cloned into the pGL3 luciferase reporter gene (Geneharma, Shanghai, China). The corresponding luciferase reporter gene vector was co-transfected with oe-ATF2 or oe-NC. Luciferase activity was determined according to the procedures of luciferase report Analysis Kit (Promega, WI, USA) after 48 h.

Chromatin immunoprecipitation (ChIP) assay

HRMECs were lysed using RIPA lysis buffer (Beyotime) and 100 μL of lysate was incubated with RIPA lysis buffer containing magnetic beads conjugated to anti-ATF2 or IgG. RNA was isolated and purified, and the content of RNA was detected by RT-qPCR.

Statistical analysis

GraphPad prism 7 software (IBM SPSS software, IL, USA) was utilized to examine the statistic. The statistic were expressed as mean ± standard deviation (all experiments were repeated for 3 times). The comparison of the two groups was evaluated by student's t-test. Furthermore, one-way ANOVA was manipulated to test the discrepancy between multiple groups. $P < 0.05$ was esteemed statistically noteworthy.

Results

USP14 knockdown inhibited proliferation, migration and angiogenesis of HG-induced HRMECs

In order to explore the role of USP14 in microvascular endothelial cells, HRMECs were treated with high glucose or mannitol. We noticed that compared with the normal group or the mannitol group, the expression of USP14 mRNA and protein was crucially up-regulated in the HG group (Fig. 1A and 1B). Then, we knocked down USP14 in HRMECs, and USP14 expression decreased significantly (Fig. 1C). We observed that USP14 expression was up-regulated in HG-induced HRMECs, while USP14 expression in DR cells with USP14 knockdown was down-regulated (Fig. 1D). The viability of HG-induced HRMECs was significantly enhanced, but USP14 knockdown in HG-induced HRMECs could effectively inhibit the viability of HRMECs (Fig. 1E). The migration ability of DR cell model was significantly enhanced, and USP14 knockdown crucially obstructed the migration of HRMECs (Fig. 1F). Tube formation assay revealed that the angiogenesis rate in the HG group increased significantly, and this phenomenon was

significantly inhibited in HG-induced HRMECs with USP14 knockdown (Fig. 1G). These results suggested that USP14 expression was abnormally up-regulated in DR cell model, while silencing USP14 crucially inhibited the migration, angiogenesis, and proliferation of HG-induced HRMECs.

USP14 regulated ATF2 expression

To study the regulation of USP14 on ATF2 in DR cell model, ATF2 expression in DR cell model was ascertained by qRT-PCR assay and Western Blot respectively. There was no obvious differentiation in ATF2 expression between normal group and mannitol group, but both of ATF2 mRNA and protein expressions were crucially up-regulated in DR cell model (Fig. 2A and 2B). Subsequently, oe-USP14 was transfected in HRMECs, and the results showed that USP14 was successfully overexpressed in HRMECs (Fig. 2C). Consistent with the above results, USP14 expression in HG-induced HRMECs was up-regulated, while USP14 expression in DR cells with oe-USP14 transfection was further up-regulated (Fig. 2D). Then, we knocked down or overexpressed USP14 in DR cell model. Silencing USP14 down-regulated the abnormally overexpression of ATF2 protein in HG-induced HRMECs, while USP14 overexpression further up-regulated ATF2 protein expression in DR cell model (Fig. 2E). IP assay revealed that USP14 could be combined with ATF2 (Fig. 2F). After HRMECs was treated with ubiquitin-proteasome inhibitor MG132 (10 μM), the protein level of ATF2 in cells was significantly up-regulated (Fig. 2G). After that, we knocked down USP14 and added protein synthesis inhibitor cycloheximide (CHX, 10 μM) in HRMECs to detect the half-life of ATF2 at different time points. We found that the degradation of ATF2 in cells with USP14 knockdown was accelerated (Fig. 2H). The above results revealed that USP14 regulated ATF2 expression in DR cell model.

ATF2 knockdown inhibited proliferation, migration, and angiogenesis of HG-induced HRMECs

With the intention of exploring the function of ATF2 in HRMECs, ATF2 was knocked down in HRMECs. Comprised with the control group, ATF2 protein level in HRMECs was down-regulated (Fig. 3A). In HG-induced HRMECs, we noticed that ATF2 expression was up-regulated, which was significantly suppressed after ATF2 knockdown (Fig. 3B). Subsequently, viability of HG-induced HRMECs was significantly increased, and ATF2 knockdown could effectively inhibit viability of DR cell model (Fig. 3C). Additionally, although the migration ability of DR cell model was significantly enhanced compared with the control group, ATF2 knockdown crucially inhibited the migration ability of HRMECs (Fig. 3D). Tube formation assay revealed that angiogenesis was increased in HG group, and ATF2 knockdown could significantly inhibit this trend (Fig. 3E). These resultants indicated that ATF2 knockdown restrained the migration, angiogenesis, and proliferation of HG-induced HRMECs.

ATF2 promoted PIK3CD expression

In order to confirm that ATF2 promoted PIK3CD expression and affected the development of DR, we first analyzed PIK3CD expression in DR cell model by qRT-PCR assay and Western blot analysis. The expressions of PIK3CD mRNA and protein were significantly up-regulated in HG-induced HRMECs (Fig. 4A and 4B). After HRMECs was transfected with oe-ATF2 plasmid, ATF2 protein level was significantly up-

regulated (Fig. 4C). Similarly, ATF2 protein was significantly up-regulated in DR cell model, and ATF2 overexpression could be further enhanced the trend (Fig. 4D). The expressions of PIK3CD mRNA and protein were down-regulated in HG-induced HRMECs with ATF2 knockdown, while the expressions of mRNA and protein were further up-regulated in HG-induced HRMECs with ATF2 overexpression (Fig. 4E and 4F). After that, dual-luciferase reporter gene assay revealed that ATF2 overexpression could significantly enhance the luciferase activity of PIK3CD-WT, but had no obvious influence on PIK3CD-MUT (Fig. 4G). Furthermore, ChIP assay showed that anti-ATF2 could enrich more PIK3CD than IgG group (Fig. 4H). These results indicated that ATF2 bound to PIK3CD and promoted its expression.

PIK3CD overexpression reversed the function of USP14 knockdown on proliferation, migration and angiogenesis of HG-induced HRMECs

In order to explore the role of PIK3CD in HRMECs, we transfected HRMECs with oe-PIK3CD plasmid and found that PIK3CD expression was crucially up-regulated (Fig. 5A). Similarly, the up-regulation trend of PIK3CD was more pronounced after transfection of oe-PIK3CD in the DR cell model (Fig. 5B). As previously mentioned, viability, migration and angiogenesis were enhanced in HG-induced HRMECs, whereas USP14 knockdown suppressed proliferation, migration and angiogenesis in the DR cell model. Furthermore, PIK3CD overexpression enhanced viability, migration and angiogenesis of DR cell model with USP14 knockdown (Fig. 5C-5E). These resultants revealed that PIK3CD overexpression attenuated the inhibitory effectiveness of USP14 knockdown on the proliferation, migration and angiogenesis of HG-induced HRMECs.

Discussion

DR is a very complex pathological process. The formation of retinal neovascularization is the most important link in the development of the disease (19, 20). Therefore, exploring the mechanism of diabetic retinal neovascularization and how to safely and limitedly inhibit neovascularization has become an important topic in DR research and clinical work.

The UPS family possesses an important function in maintaining protein homeostasis and is associated with diabetes-related complications (21, 22). In the study of type 2 diabetes, Forand et al. found that inhibiting the dissociation of USP7/Insulinreceptorsubstrate1 (IRS1) and preventing the ubiquitination of IRS1 had a protective effect on diabetic mice (23). Additionally, it was observed that USP9X played a protective role in diabetic nephropathy by stabilizing de-ubiquitin connexin43 (Cx43) expression (24). USP22 overexpression was observed in podocytes induced by high glucose, and silencing USP22 could alleviate the cytotoxicity of podocytes (25). Moreover, USP14 overexpression participated in the development of diabetic retinopathy by inducing deubiquitination of transforming growth factor-β-1 (TβR1) (11). In this study, USP14 and its downstream protein ATF2 were abnormally overexpressed in HG-induced HRMECs, and USP14 directly interacted with ATF2 and prevented the degradation of ATF2. USP14 knockdown inhibited the proliferation, migration and angiogenesis of HRMECs upon high glucose.

ATF2 is a member of ATF/CREB bZIP transcription factor family. In a study of ovarian cancer, Yi et al. found that ATF2 might be involved in the exocrine function of angiogenesis (26). Furthermore, Zhao et al. found that 15 (S)-HETE activated ATF2 in HRMECs and led to angiogenesis and differentiation (27). Recently, Wang et al. claimed that ATF2 played an important role in VEGF-induced retinal neovascularization, and ATF2 knockdown alleviated VEGF-induced angiogenesis and reduced HRECs migration ability (28). In this study, we also observed a similar phenomenon in the DR cell model, that is, ATF2 knockdown inhibited the proliferation, migration and angiogenesis of HRMECs. Additionally, it is worth noting that ATF2 could bound to PIK3CD. Along with ATF2 overexpression, PIK3CD expression was also up-regulated in DR cell model.

In the occurrence and development of diabetes, continuous hyperglycemia promotes PI3K pathway activation, and finally accelerates the development of DR (29). PI3K/Akt signal pathway is a key signal pathway to induce endothelial cell proliferation and angiogenesis (30). In an *in vitro* study of diabetic retinopathy, Wang et al. found that up-regulation of miR-199a-3p inhibited PI3K/Akt signaling pathway, thereby improving HG-stimulated HRMECs angiogenesis (31). Qiu et al. inhibited PI3K/Akt pathway through recombinant human manspin and attenuated proliferation, oxidative stress and angiogenesis in HRMECs upon high glucose (32). PI3Kδ is an important member of the PI3K family, which is encoded and synthesized by PIK3CD gene (33). Wu et al. confirmed that PI3Kδ expression was up-regulated in DR cell model, which activated Akt signal pathway and aggravated the progress of DR (19). Our results confirmed this finding. PIK3CD expression was up-regulated in DR cell model. Furthermore, PIK3CD overexpression attenuated the inhibitory effectiveness of USP14 knockdown on the proliferation, migration and angiogenesis of HG-induced HRMECs.

In brief, these evidences pointed to USP14 regulating the ATF2/PIK3CD axis to promote the proliferation, migration and angiogenesis of HRMECs upon high glucose. Although this study temporarily stayed at molecular mechanism, it provided a new idea and experimental basis for the clinical treatment of diabetic retinopathy.

Abbreviations

Diabetic retinopathy: DR;

High glucose: HG;

Human retinal microvascular endothelial cells: HRMECs;

Chromatin immunoprecipitation: ChIP;

Vascular endothelial growth factor: VEGF;

Ubiquitin-proteasome system: UPS;

Deubiquitinating enzyme: DUB;

Ubiquitin-specific protease 14: USP14;

Activating transcription factor 2: ATF2;

Phosphoinositide-3 kinase catalytic subunit δ: PI3Kδ, or PIK3CD;

Cell Counting Kit-8: CCK-8;

Fetal bovine serum: FBS;

Phosphate buffered saline: PBS;

Quantitative real-time PCR: qRT-PCR;

Poly vinylidene difluoride filter: PVDF;

Sodium dodecyl sulfate-polyacrylamide gel electrophoresis: SDS-PGE.

Declarations

Ethics approval and consent to participate

Not applicable.

Competing interests

The authors declare that they have no conflict of interest.

Funding

Not applicable.

Authors' contributions

Fu-Tao He: Formal analysis; Investigation; Resources; Data Curation;

Xiao-Lin fu: Conceptualization; Methodology; Validation;

Mo-Han Li: Writing - Original Draft;

Chun-Yan Fu: Visualization; Supervision;

Jian-Zhi Chen: Writing - Review & Editing; Project administration; Funding acquisition

References

1. Bek T. Arterial Oxygen Saturation in Neovascularizations in Proliferative Diabetic Retinopathy. Retina. 2018;38(12):2301–8.
2. Yao L, Zhong Y, He L, Wang Y, Wu J, Geng J, et al. Serum CA125 Level Is Associated with Diabetic Retinopathy in Chinese Patients with Type 2 Diabetes. Diabetes Metab Syndr Obes. 2020;13:1803–12.
3. Singer MA, Kermany DS, Waters J, Jansen ME, Tyler L. Diabetic macular edema: it is more than just VEGF. F1000Res. 2016;5.
4. Dumitrescu AG, Istrate SL, Iancu RC, Guta OM, Ciuluvica R, Voinea L. Retinal changes in diabetic patients without diabetic retinopathy. Rom J Ophthalmol. 2017;61(4):249–55.
5. Niestrata-Ortiz M, Fichna P, Stankiewicz W, Stopa M. Enlargement of the foveal avascular zone detected by optical coherence tomography angiography in diabetic children without diabetic retinopathy. Graefes Arch Clin Exp Ophthalmol. 2019;257(4):689–97.
6. Mines MA, Goodwin JS, Limbird LE, Cui FF, Fan GH. Deubiquitination of CXCR4 by USP14 is critical for both CXCL12-induced CXCR4 degradation and chemotaxis but not ERK ativation. J Biol Chem. 2009;284(9):5742–52.
7. Kim HT, Goldberg AL. The deubiquitinating enzyme Usp14 allosterically inhibits multiple proteasomal activities and ubiquitin-independent proteolysis. J Biol Chem. 2017;292(23):9830–9.
8. Liu B, Zhang Z, Hu Y, Lu Y, Li D, Liu J, et al. Sustained ER stress promotes hyperglycemia by increasing glucagon action through the deubiquitinating enzyme USP14. Proc Natl Acad Sci U S A. 2019;116(43):21732–8.
9. Liu B, Jiang S, Li M, Xiong X, Zhu M, Li D, et al. Proteome-wide analysis of USP14 substrates revealed its role in hepatosteatosis via stabilization of FASN. Nat Commun. 2018;9(1):4770.
10. Lundgren S, Odrzywol E. USP14 inhibitors as potential anticancer agents. Future Med Chem. 2018;10(15):1741–3.
11. Fu S, Zheng Y, Sun Y, Lai M, Qiu J, Gui F, et al. Suppressing long noncoding RNA OGRU ameliorates diabetic retinopathy by inhibition of oxidative stress and inflammation via miR-320/USP14 axis. Free Radic Biol Med. 2021;169:361–81.
12. Jiang N, Wang X, Xie X, Liao Y, Liu N, Liu J, et al. lncRNA DANCR promotes tumor progression and cancer stemness features in osteosarcoma by upregulating AXL via miR-33a-5p inhibition. Cancer Lett. 2017;405:46–55.
13. Lin Z, Qu S, Peng W, Yang P, Zhang R, Zhang P, et al. Up-Regulated CCDC34 Contributes to the Proliferation and Metastasis of Hepatocellular Carcinoma. Onco Targets Ther. 2020;13:51–60.
14. Shao Y, Dong LJ, Takahashi Y, Chen J, Liu X, Chen Q, et al. miRNA-451a regulates RPE function through promoting mitochondrial function in proliferative diabetic retinopathy. Am J Physiol Endocrinol Metab. 2019;316(3):E443-E52.
15. Geng M, Yang Y, Cao X, Dang L, Zhang T, Zhang L. Targeting CDK12-mediated transcription regulation in anaplastic thyroid carcinoma. Biochem Biophys Res Commun. 2019;520(3):544–50.

16. Foukas LC, Berenjeno IM, Gray A, Khwaja A, Vanhaesebroeck B. Activity of any class IA PI3K isoform can sustain cell proliferation and survival. Proc Natl Acad Sci U S A. 2010;107(25):11381–6.
17. Colomiere M, Permezel M, Riley C, Desoye G, Lappas M. Defective insulin signaling in placenta from pregnancies complicated by gestational diabetes mellitus. Eur J Endocrinol. 2009;160(4):567–78.
18. Wu W, Zhou G, Han H, Huang X, Jiang H, Mukai S, et al. PI3Kdelta as a Novel Therapeutic Target in Pathological Angiogenesis. Diabetes. 2020;69(4):736–48.
19. Arrigo A, Aragona E, Bandello F. VEGF-targeting drugs for the treatment of retinal neovascularization in diabetic retinopathy. Ann Med. 2022;54(1):1089–111.
20. Du MR, Yan L, Li NS, Wang YJ, Zhou T, Jiang JL. Asymmetric dimethylarginine contributes to retinal neovascularization of diabetic retinopathy through EphrinB2 pathway. Vascul Pharmacol. 2018;108:46–56.
21. Lu L, Ma J, Liu Y, Shao Y, Xiong X, Duan W, et al. FSTL1-USP10-Notch1 Signaling Axis Protects Against Cardiac Dysfunction Through Inhibition of Myocardial Fibrosis in Diabetic Mice. Front Cell Dev Biol. 2021;9:757068.
22. Mao R, Shen J, Hu X. BMSCs-derived exosomal microRNA-let-7a plays a protective role in diabetic nephropathy via inhibition of USP22 expression. Life Sci. 2021;268:118937.
23. Forand A, Koumakis E, Rousseau A, Sassier Y, Journe C, Merlin JF, et al. Disruption of the Phosphate Transporter Pit1 in Hepatocytes Improves Glucose Metabolism and Insulin Signaling by Modulating the USP7/IRS1 Interaction. Cell Rep. 2016;16(10):2736–48.
24. Sun XH, Xiao HM, Zhang M, Lin ZY, Yang Y, Chen R, et al. USP9X deubiquitinates connexin43 to prevent high glucose-induced epithelial-to-mesenchymal transition in NRK-52E cells. Biochem Pharmacol. 2021;188:114562.
25. Shi JX, Wang QJ, Li H, Huang Q. Silencing of USP22 suppresses high glucose-induced apoptosis, ROS production and inflammation in podocytes. Mol Biosyst. 2016;12(5):1445–56.
26. Yi H, Ye J, Yang XM, Zhang LW, Zhang ZG, Chen YP. High-grade ovarian cancer secreting effective exosomes in tumor angiogenesis. Int J Clin Exp Pathol. 2015;8(5):5062–70.
27. Zhao T, Wang D, Cheranov SY, Karpurapu M, Chava KR, Kundumani-Sridharan V, et al. A novel role for activating transcription factor-2 in 15(S)-hydroxyeicosatetraenoic acid-induced angiogenesis. J Lipid Res. 2009;50(3):521–33.
28. Wang R, Xu Y, Niu C, Gao X, Xu X. A Novel Small Peptide H-KI20 Inhibits Retinal Neovascularization Through the JNK/ATF2 Signaling Pathway. Invest Ophthalmol Vis Sci. 2021;62(1):16.
29. Tang L, Zhang C, Lu L, Tian H, Liu K, Luo D, et al. Melatonin Maintains Inner Blood-Retinal Barrier by Regulating Microglia via Inhibition of PI3K/Akt/Stat3/NF-kappaB Signaling Pathways in Experimental Diabetic Retinopathy. Front Immunol. 2022;13:831660.
30. Di Y, Zhang Y, Yang H, Wang A, Chen X. The mechanism of CCN1-enhanced retinal neovascularization in oxygen-induced retinopathy through PI3K/Akt-VEGF signaling pathway. Drug Des Devel Ther. 2015;9:2463–73.

31. Wang L, Liu WX, Huang XG. MicroRNA-199a-3p inhibits angiogenesis by targeting the VEGF/PI3K/AKT signalling pathway in an in vitro model of diabetic retinopathy. Exp Mol Pathol. 2020;116:104488.
32. Qiu F, Tong H, Wang Y, Tao J, Wang H, Chen L. Recombinant human maspin inhibits high glucose-induced oxidative stress and angiogenesis of human retinal microvascular endothelial cells via PI3K/AKT pathway. Mol Cell Biochem. 2018;446(1–2):127–36.
33. Fransson S, Uv A, Eriksson H, Andersson MK, Wettergren Y, Bergo M, et al. p37delta is a new isoform of PI3K p110delta that increases cell proliferation and is overexpressed in tumors. Oncogene. 2012;31(27):3277–86.

Figures

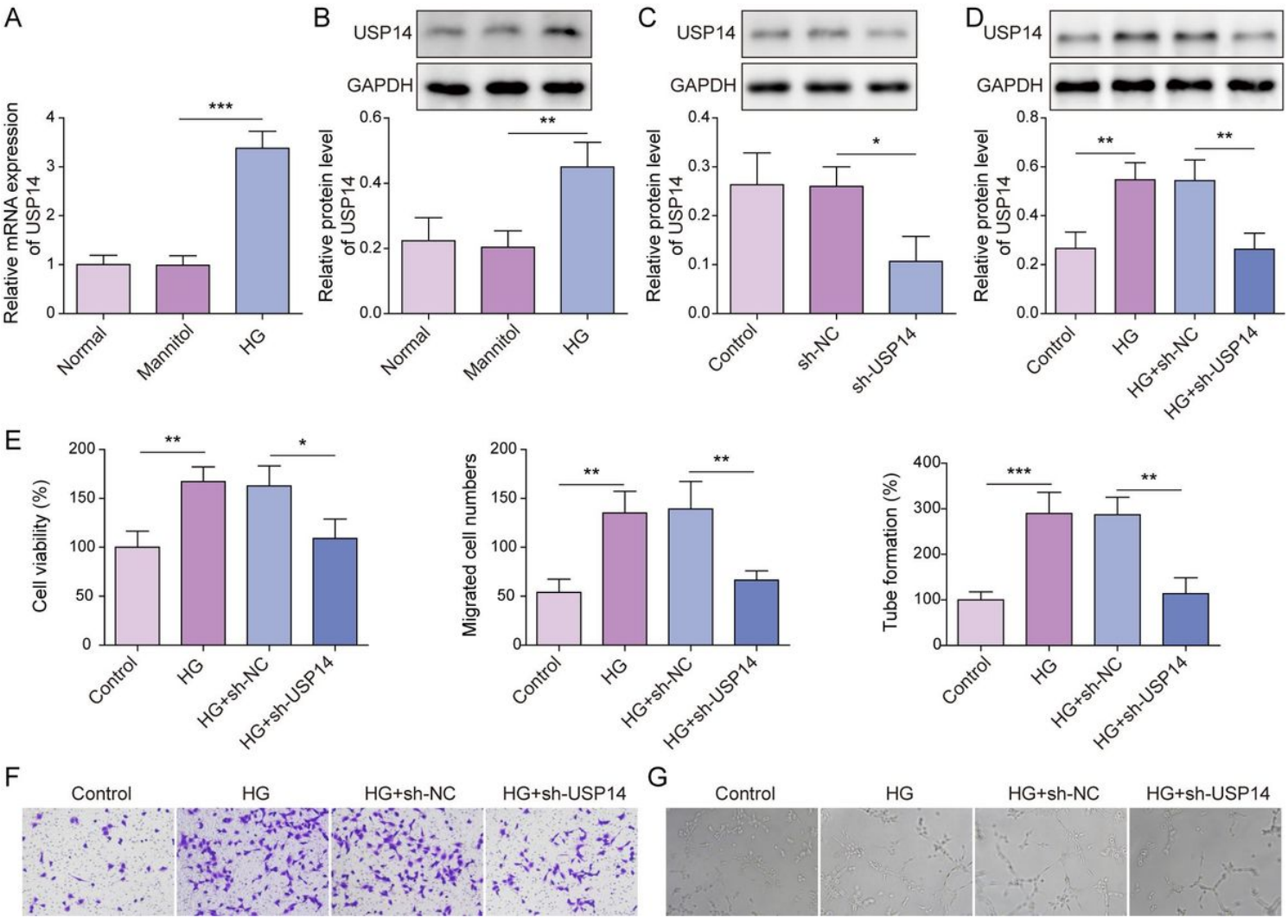

Figure 1

USP14 knockdown inhibited proliferation, migration and angiogenesis of HG-induced HRMECs.

DR cell model was constructed using HRMECs treated with 30 mmol/L glucose medium, and sh-USP14 was transfected into HG-induced HRMECs. (A-D) USP14 expression was ascertained by qRT-PCR assay and western blot. (E) HRMECs viability was determined by CCK-8 assay. (F) HRMECs migration ability was ascertained by Transwell assay. (G) HRMECs angiopoiesis was ascertained by Tube formation assay. Each group performed 3 independent experiments leastwise. **P < 0.05, **P < 0.01, ***P < 0.001*.

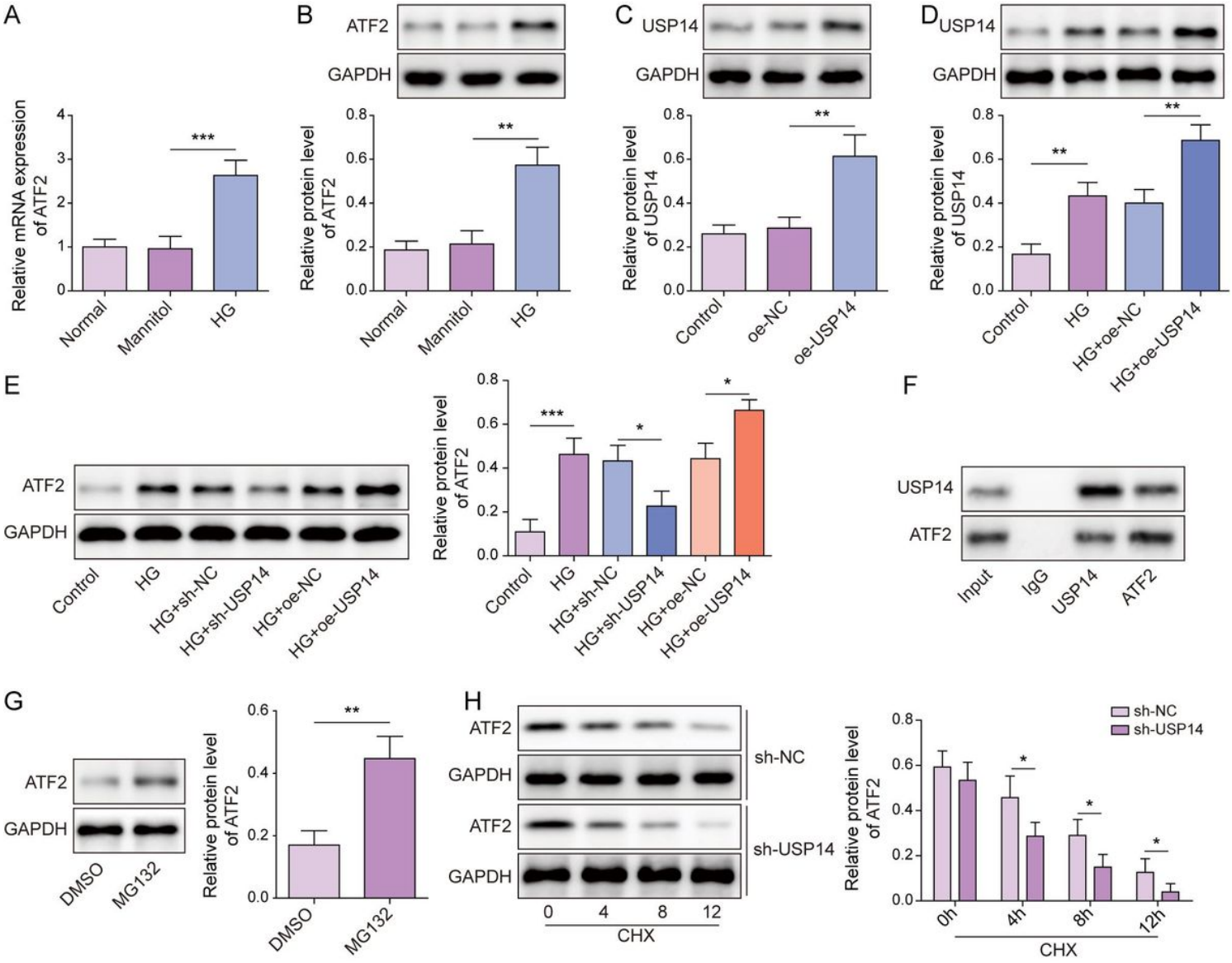

Figure 2

USP14 regulated ATF2 expression.

Sh-USP14 or oe-USP14 was transfected into HG-induced HRMECs. (A-B) ATF2 expression was ascertained by qRT-PCR assay and western blot. (C-D) USP14 expression was detected by western blot. (E) ATF2 expression was ascertained by western blot. (F) IP was manipulated to confirm the relationship of USP14 and ATF2. (G-H) ATF2 expression was detected by western blot in HG-induced HRMECs with MG132 or CHX. Each group performed 3 independent experiments leastwise. **P < 0.05, **P < 0.01, ***P < 0.001*.

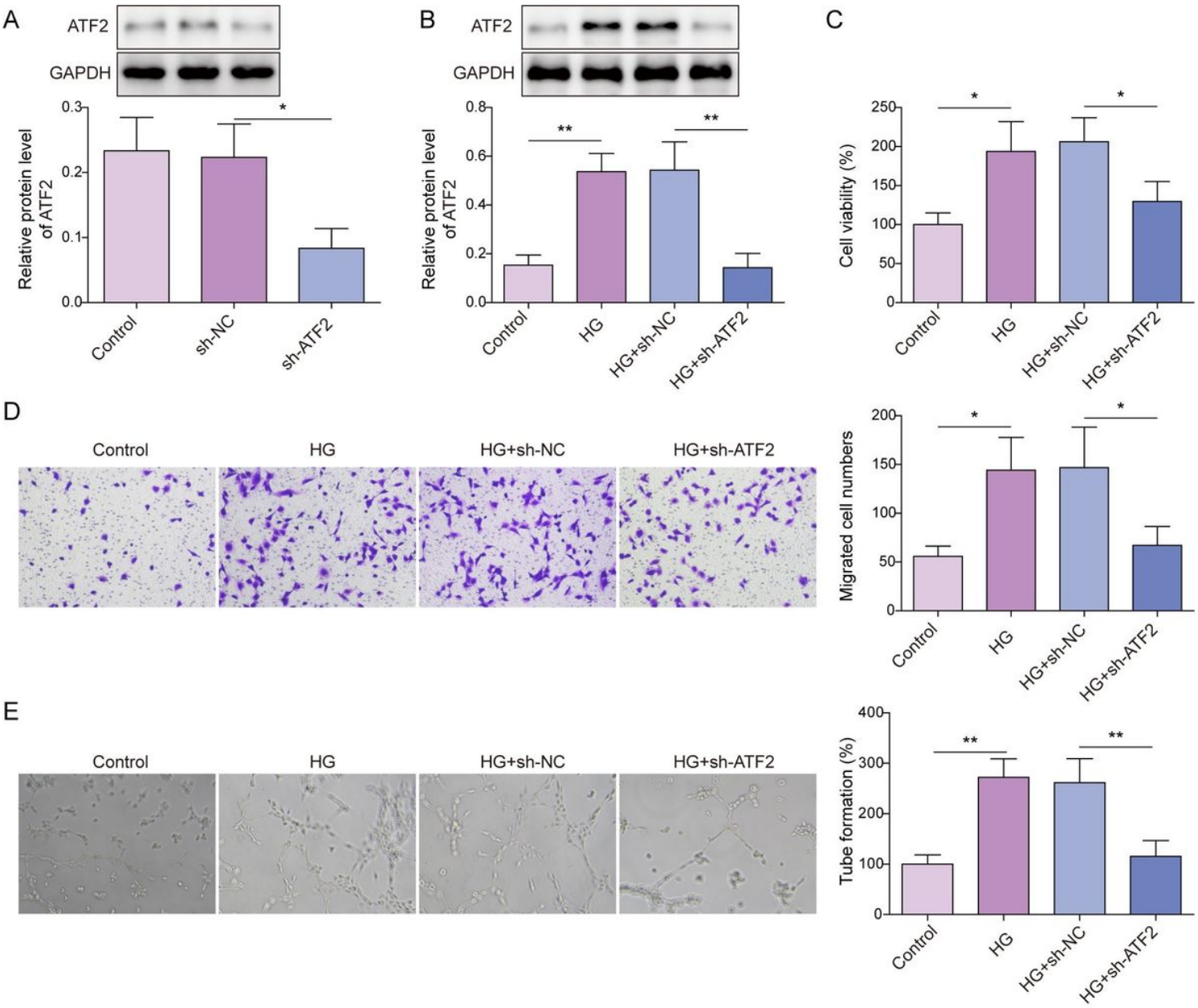

Figure 3

ATF2 knockdown inhibited proliferation, migration, and angiogenesis of HG-induced HRMECs.

Sh-ATF2 was transfected into HG-induced HRMECs. (A-B) ATF2 expression was detected by western blot. (C) The HRMECs viability was determined by CCK-8 assay. (D) HRMECs migration ability was ascertained by Transwell assay. (E) The HRMECs angiopoiesis was ascertained by Tube formation assay. Each group performed 3 independent experiments leastwise. *P < 0.05, **P < 0.01, ***P < 0.001.

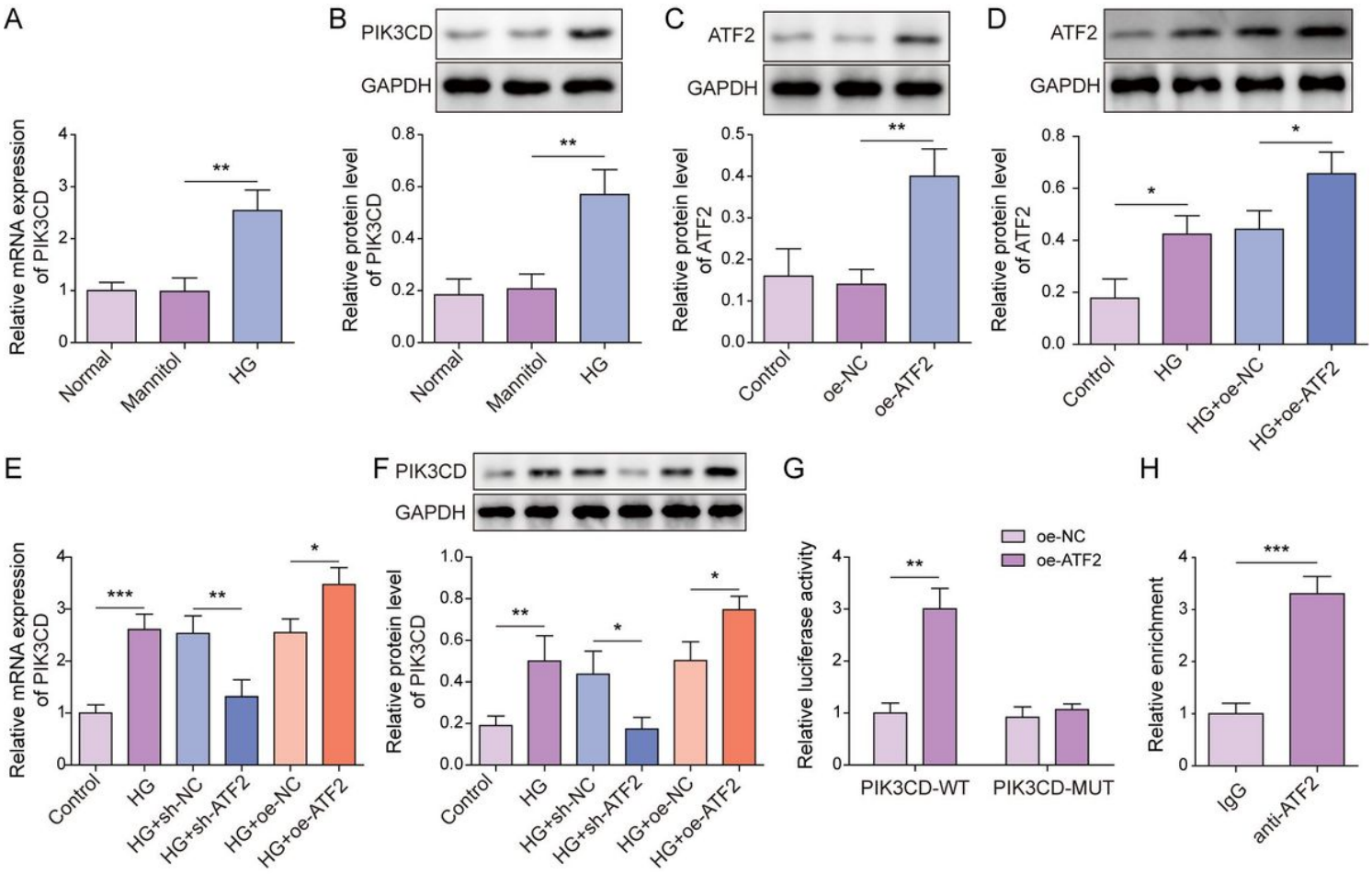

Figure 4

ATF2 promoted PIK3CD expression.

Sh-ATF2 or oe-ATF2 was transfected into HG-induced HRMECs. (A-B) PIK3CD expression was ascertained by qRT-PCR assay and western blot. (C-D) ATF2 expression was detected by western blot. (E-F) PIK3CD expression was ascertained by qRT-PCR assay and western blot. (G-H) Dual-luciferase reporter assay and ChIP assay were manipulated to confirm the relationship of ATF2 and PIK3CD. Each group performed 3 independent experiments leastwise. **P < 0.05, **P < 0.01, ***P < 0.001.*

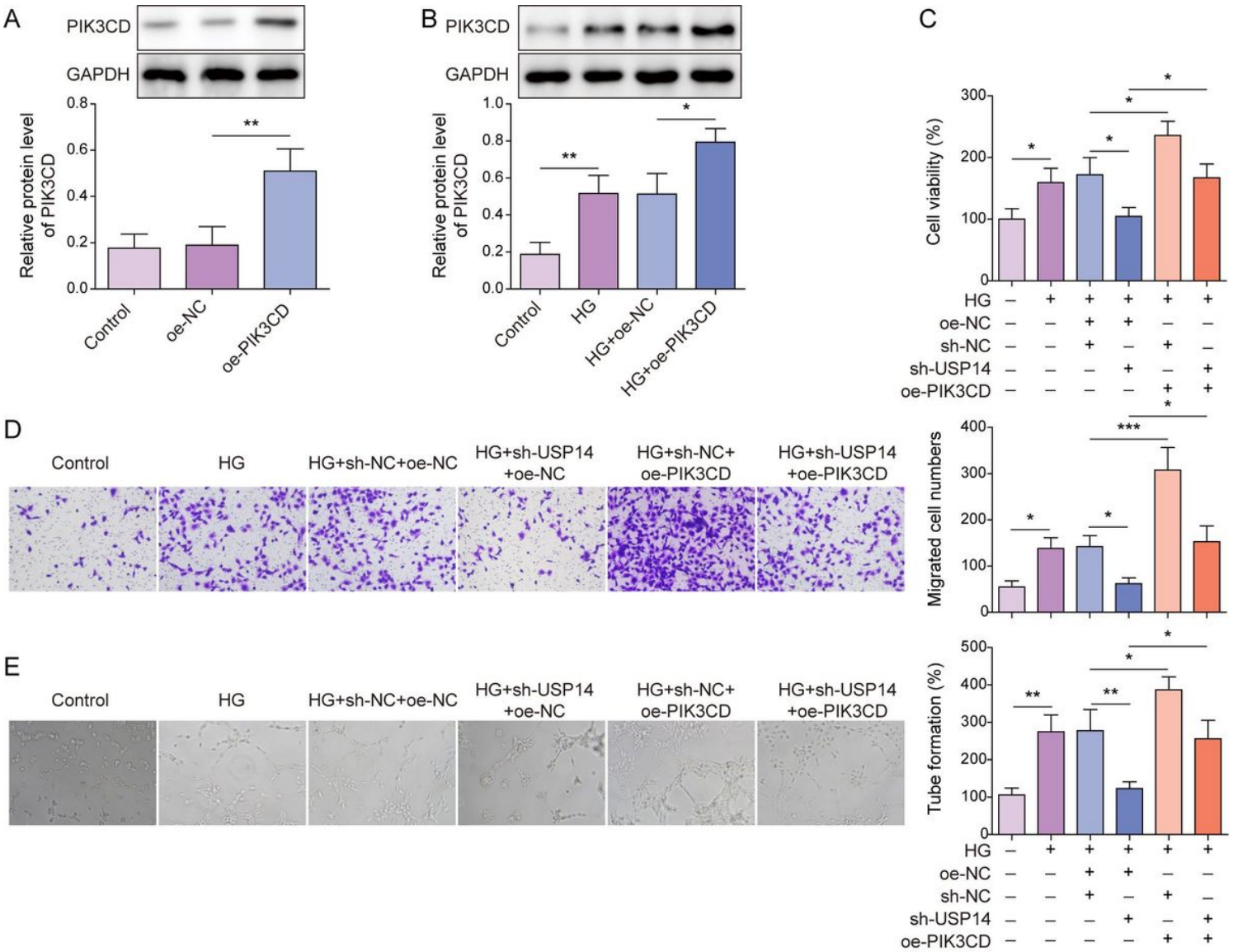

Figure 5

PIK3CD overexpression reversed the function of USP14 knockdown on proliferation, migration and angiogenesis of HG-induced HRMECs.

Sh-USP14 and/or oe-PIK3CD were transfected into HG-induced HRMECs. (A-B) PIK3CD expression was ascertained by western blot. (C) The HRMECs viability was determined by CCK-8 assay. (D) HRMECs migration ability was ascertained by Transwell assay. (E) The HRMECs angiopoiesis was ascertained by Tube formation assay. Each group performed 3 independent experiments leastwise. **P < 0.05, **P < 0.01, ***P < 0.001.*